A Pseudoatom Approach to Molecular Truncation: Application in ab Initio MBPT Methods

DeCarlos E. Taylor* and Steven W. Bunte†

U.S. Army Research Laboratory, Aberdeen Proving Ground, Maryland 21005

Keith Runge

Department of Physics, University of Florida, Gainesville, Florida 32611

Received: September 12, 2005; In Final Form: March 20, 2006

In this paper, we test the performance of the molecular truncation method of Mallik et al.,[1] which was originally applied at the semiempirical NDDO level, in ab initio MBPT methods. Pseudoatoms developed for the replacement of $-OCH_3$ and $-OCH_2CH_3$ functional groups are used in optimizations of selected clusters, and the resulting geometries are compared to reference values taken from the full molecules. It is shown that the pseudoatoms, which consist of parametrized effective core potentials for the nearest neighbor interactions and an external charge field for long-range Coulomb effects, perform well at the MP2 and CCSD levels of theory for the suite of molecules to which they were applied. Representative timings for some of the pseudoatom-terminated clusters are presented, and it is seen that there is a significant reduction in computational time, yet the geometric configurations and deprotonation energies of the pseudoatom-terminated clusters are comparable to the more computationally expensive all-atom molecules.

Introduction

Despite the rapid improvements to computer technology in regards to processor speed and available storage, the application of ab initio post-Hartree−Fock quantum mechanics (QM) methods to large molecules remains a difficult challenge for the computational chemistry community. Techniques such as the "divide and conquer"[2] or conjugate gradient density matrix search algorithms[3] have brought Hartree−Fock and density functional (DFT) levels of theory to a linear dependence on the system size. Correlated models such as many body perturbation theory[4] (MBPT) or coupled cluster (CC) methods[5] have also been shown to scale linearly[6,7] when used in conjunction with an orbital localization procedure. In addition, the fragment molecular orbital method has been applied at the CC level of theory to systems with over 3600 basis functions and shown to scale very efficiently.[8] However, in their standard implementation using a canonical molecular orbital basis, the computational cost of correlated models such as MBPT or CC theory suffer from at least fifth-order scaling, which limits their application to large systems.

Many strategies have been formulated in an attempt to circumvent the size limitation problem. Although the proposed methods differ in technique, all of the schemes require a partitioning of the full system into a QM region where high level methods will be applied and a "remainder", which will (1) be treated explicitly with a lower level model or (2) be neglected completely but have its effects on the QM region modeled by an effective interaction. Perhaps the most widely used technique of type 1 is a coupling of QM methods with those of molecular mechanics (MM).[9] In this approach, a region of interest is treated with a high level of theory and the remaining, chemically inert, portions of the system are treated with a MM force field.[10] The major difficulty in the QM/MM type methods is accurately coupling the QM and MM portions across the boundary that divides the two regions. There have been many suggestions concerning an appropriate coupling of the two regions ranging from a simple inclusion of hydrogen link atoms[11] that terminate dangling QM bonds to schemes that include localized frozen orbitals[12] and/or effective group potentials[13] obtained from smaller model compounds. The utter simplicity of the link atom method is highly desirable; however, a major drawback is that it introduces artificial interactions into the system.[14] On the contrary, the localized orbital and effective group potential schemes have shown promise; however, they are somewhat cumbersome to implement and apply in general quantum chemistry software packages without a significant amount of programming.

Another technique that has proven beneficial for truncation of large molecules is the inclusion of pseudoatoms (pseudobonds) to cap the bonds at the boundary of the QM region. In this approach, which has been developed for semiempirical[15] as well as ab initio models,[16] a larger functional group consisting of several atoms is replaced by a single "effective" atom that is designed to mimic the behavior of the larger fragment that it replaces. Zhang et al.,[16] working at the DFT level, developed a pseudoatom that replaced the four atoms in a methyl group by a single atomic entity. In that work, a methyl group in ethane was replaced by a valence electron only fluorine atom to which an effective core potential (ECP) was assigned. The coefficients and exponents that parametrize the fluorine ECP were then optimized such that the properties of the remaining methyl in the $F-CH_3$ fragment matched those from the full ethane molecule. The pseudoatom, developed in this way, was then used to replace methyl groups across C−C bonds in larger

* Corresponding author. U.S. Army Research Laboratory, Propulsion Science Branch, Aberdeen Proving Ground, MD 21005. Tel: 410-306-0853. Fax: 410-306-1909. E-mail: decarlos.taylor@us.army.mil.

† E-mail: bunte@arl.army.mil.

10.1021/jp055149h CCC: $33.50
Published on Web 04/27/2006

molecules. B3LYP/MM geometry optimizations using the pseudoatom at the boundary resulted in standard deviations of 0.017 Å for bond lengths and 0.015° for bond angles as compared to results using full QM treatments. A similar approach was applied by DiLabio et al.;[17] however, in their work they generated a four-electron ECP for carbon and subsequently added terms to their potential to shift three of the four valence electrons into the core. This approach has the advantage that fewer electrons need explicit treatment in the QM calculation as compared to the seven valence electron fluorine of Zhang et al. Their ECP was then adjusted so that the structure and atomic charges of the remaining methyl group matched those from the full ethane molecule, analogous to the work of Zhang et al. The pseudoatom was then used to compute protonation energies for histidine where a nine-atom side chain was replaced by a single pseudoatom. It was found that the protonation energies showed good agreement with results from the full molecule.

The work of Zhang et al.[16] and DiLabio et al.[17] indicates that the parametrized ECP pseudoatoms are a convenient way to introduce the inductive effects of large substituents into the QM region of a truncated molecule. This type of scheme is also of value to the molecular dynamics (MD) community, which routinely conducts simulations containing numbers of particles far beyond the limits of ab initio quantum chemistry.[18] However, because of the inherent limitations in the potentials that drive the MD simulations, truly quantitative results cannot be obtained directly. Instead, after an MD run, simulators often identify sites of interest and apply ab initio QM to small clusters extracted from the final configuration of the MD run.[19] Treated in this manner, the effects of the surrounding surface on the cluster are completely neglected; however, the pseudoatom scheme, as shown in other work by DiLabio et al.[20] during studies of silicon clusters extracted from silicon surface models, may be of some value. In that work, a silicon pseudoatom was used to terminate small silicon clusters used to model extended silicon surfaces. The resulting ionization potential, electron affinity, and HOMO−LUMO gap resulting from the pseudoatom-terminated clusters showed much better agreement with values from the extended system than did hydrogen-atom-terminated clusters, which is indicative of the pseudoatom's ability to effectively represent the important inductive effects of larger functional groups although the results did indicate a slight dependence on cluster size.

In a similar study, Mallik et al.,[1] working in the context of semiempirical (NDDO) theory, developed a pseudoatom for use in extended silica systems. Using fluorine, the pseudoatom was determined by varying the parameters contained in the AM1 Hamiltonian such that the geometry and forces in a truncated silica cluster matched those from the full molecule. This pseudoatom was then used to truncate a small three-membered silica ring and a 108-atom silica nanorod.[21] For the latter, the system size was reduced to only 24 atoms (12 Si−O and 12 pseudoatoms), resulting in a significant reduction in computational cost. The use of pseudoatoms by Mallik et al. to truncate extended surfaces is similar in spirit to that of DiLabio's[20] treatment of silicon surfaces. However Mallik et al. added an additional component to their truncation scheme whereby the long-range Coulomb interactions from the bulk environment were included self-consistently in the QM calculation via interaction of the QM subsystem with the electric dipole generated by the surrounding charge distribution from the truncated region. The results demonstrated that the parametrized pseudoatom, in conjunction with the dipole from the surrounding region, gave the best results as compared to the use of pseudoatoms alone. The success of the pseudoatom + dipole technique for the small ring suggests that it may be a useful tool for ab initio methods as well.

Mallik et al. focused on generating pseudoatoms for oxygen atoms linked to silicon. Because we intend to extend that work for systems of biological interest, we have begun by considering minimum energy geometries for systems including oxygen linked to alkyl groups that also include heteroatoms of general biological interest. For our initial studies we have chosen to look at ethers and phosphoethers so that the extension of these calculations into biologically relevant macromolecules, like DNA, can be built up from the pseudoatom database that we are developing. Further, we have an interest in the rate of chemical reactions of large biological molecules and particularly in a constructive investigation of the role of reactive radicals present in biological systems. An accurate prediction of rate constants requires accurate structures for both minimum energy and transition-state configurations, both of which can be determined to chemical accuracy with MBPT/CC methods.[22] For the larger sized molecules, the MBPT/CCSD methods have proven to be computationally costly because of the number of heavy atoms present in these molecules. Further, the increase in the 3N-6 internal degrees of freedom contributed by the bulky alkoxy side chains, which may oscillate from one optimization cycle to the next, particularly during transition-state searches, increases the number of optimization steps (and CPU time) required to locate stationary points, which is somewhat superfluous given that these units have a small effect on the chemistry of the reactive regions upon which we are focused.

In this paper we report an implementation of the Mallik et al. pseudoatom truncation scheme, which can be used in conjunction with ab initio MBPT and CC methods. Specifically, we present pseudoatoms that can be used to replace $O-CH_3$ (*o*-methyl) and $O-CH_2-CH_3$ (*o*-ethyl) functional groups. Following a description of the procedures used to parametrize the effective core potential of the pseudoatom and assign the external charge field from the truncated region, a comparison of geometries from several truncated clusters to their all-atom counterparts is presented. It will be seen that the pseudoatom, coupled with the associated external field from the truncated portion, results in a smaller sized system that must be treated with QM yet yields geometries of similar quality to calculations on the full molecule. This suggests that the pseudoatom-external field approach can be an effective means of reducing the computational cost of ab initio methods.

Method

To develop a pseudoatom representative of *o*-methyl groups, we used as our reference cluster dimethyl ether $(H_3C)-O-(CH_3)$ where the equilibrium geometry was obtained at the MP2/6-311++G** level of theory (all QM calculations were performed with the ACES II[23] program package). Using dimethyl ether (DME), an $O-CH_3$ linkage was replaced by a valence-electron-only fluorine atom (Figure 1) to which an ECP of the usual form

$$V_L(r) = \sum_i r^{\alpha_{iL}} c_{iL} e^{-\zeta_{iL} r^2} \qquad (1)$$

was assigned where L ranges from 0 to the maximum angular momentum of the basis set.

Attempts at using other types of atoms in lieu of fluorine were made; however, it was found that the convergence of the Hartree−Fock equations was less problematic when fluorine

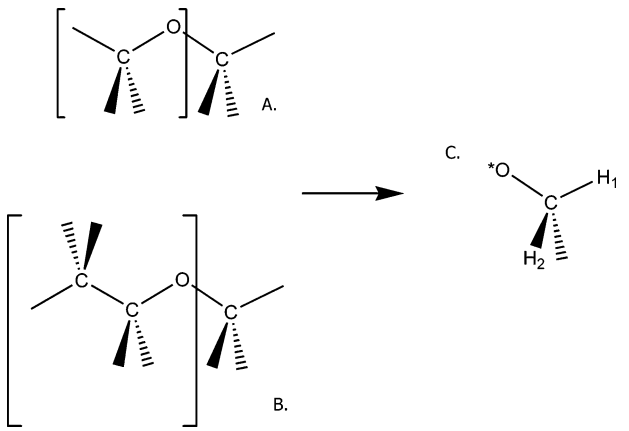

Figure 1. Dimethyl ether (A), methyl ethyl ether (B), reference molecules, and truncated portions (atoms in brackets) for each system. The resulting fragment with pseudoatom is shown in C.

was used. The fluorine 6-31G basis set was used on the pseudoatom; however, the remaining carbon/hydrogen atoms in the truncated cluster retained the 6-311++G** basis used in the full molecule. Pseudoatoms that included d-type functions were explored; however, the polarization functions were found to offer little improvement over the (s,p) basis variants. Therefore, the smaller basis was chosen to minimize computational scaling. At present we have chosen not to develop pseudoatom-specific basis sets as did Zhang[24] who, following his original formulation, later extended the parametrization of his pseudoatom to include functional-group-specific basis sets as well as effective core potentials.

Given the functional form of the ECP in eq 1, before the parametrization of the exponents and coefficients of the ECP can ensue, it is necessary to determine the location/orientation of the methyl group dipole, which is the lead term in a multipole expansion of the long-range Coulomb interaction because the monopole vanishes due to charge neutrality of our subsystems. In practice, based on a simple population analysis, there is a small amount of charge transfer from the functional group to the heteroatom to which it is bonded. Therefore, the external field of the functional group is represented by two point charges of opposite sign where the magnitude of the positive charge is equal to the total positive charge contained in the functional group being replaced (9 for methyl, 17 for ethyl). This charge is located at the center of positive charge of the truncated functional group using the coordinates of the truncated atoms in the MP2 minimum energy configuration of the full molecule. The magnitude and location of the negative charge is determined by an analysis of the MP2 density. Specifically, we partition the density in the region of the methyl group that we are modeling into small cubes whose volume is typically on the order of 0.1 Å^3 or less. We assume that the density is constant within each cube. Treated in this manner, the total negative charge within each cube, q_i, is given by

$$q_i = -p(r_i)*V \tag{2}$$

where $p(r_i)$ is the value of the MP2 density in the ith cube and V is the volume. The number of cubes is then increased continually until the total negative charge converges and shows no appreciable difference upon addition of more cubes. In this manner, the charge transfer that may occur with differing functional groups may be properly accounted for because the magnitude of the negative charge is computed from an analysis of the density within the functional group. Once the total negative charge has converged, the location of the center of negative charge can be computed from the charges within, and locations of, the cubes that define the final grid. Given the magnitude and position of the two centers of charge that constitute the external field, during the MP2 or CCSD geometry optimizations of the truncated clusters, the external field interacts with the real atoms through the $-Z/r$ term of the core Hamiltonian and also contributes attractive and repulsive interactions to the Born−Oppenheimer additive constant.

TABLE 1: Orientation and Magnitude of Positive(Negative) Point Charges for *o*-Methyl and *o*-Ethlyl Pseudoatoms[a]

fragment	R	Θ	Φ	Q
o-methyl	1.539(1.566)	111.4(115.3)	180(180)	9.0(−8.89)
o-ethyl	1.894(1.948)	135.3(135.5)	180(180)	17.0(−16.88)

[a] With respect to the fragment and atomic labeling depicted in Figure 1C, R is the distance (Å) of the point charge from the O* nucleus, Θ is the point charge −O*−carbon angle, and Φ is the dihedral angle subtended by the point-charge −O*−carbon−H(1) atoms. Q is the magnitude of the charge.

TABLE 2: Gaussian Expansions for *o*-Methyl and *o*-Ethyl Pseudoatoms Corresponding to the Symbols Given in Equation 1

L	α	ς	C (*o*-methyl)	C (*o*-ethyl)
1	1	51.0221232	−9.3442891	−10.3442891
0	0	42.4567298	1.7659890	1.7659890
0	2	71.5434024	5.4482869	5.4482869

Using this procedure, point charges representative of *o*-methyl and *o*-ethyl fragments were determined using DME and methyl ethyl ether (Figure 1) molecules, respectively. The magnitude and orientation of the point charges that result from the above analysis are given for each moiety in Table 1. Note that the standard ACES II program system does not contain a facility for defining an external point-charge field; therefore, modifications of the input and Gaussian integral subroutines were made in order to conduct this study.

A. Parametrization and Analysis of Pseudoatom. Given the location of the centers of charge for the *o*-methyl and *o*-ethyl fragments, the ACES II program suite was interfaced with a quasi-Newton[25] and a genetic algorithm[26] to determine the best-fit parameters in the fluorine ECP. Using the optimization algorithms, the function f, given by

$$f = \sum_i \omega_i (s_i^{\text{fragment}} - s_i^{\text{full}})^2 \tag{3}$$

where s corresponds to the internal coordinate bonds, angle, and dihedrals for the fragment and full molecules, was minimized, that is, the exponents and coefficients for the fluorine ECP were optimized such that the geometry of the fragment in Figure 1 matched that from the full DME or methyl ethyl ether reference molecules computed at the MP2 level of theory. ω_i in eq 3 is an arbitrary weight factor, typically chosen to be unity for most points. The converged ECP parameters for the two pseudoatoms are contained in Table 2, and a comparison of optimized internal coordinates from the fragment and reference molecules are shown in Table 3. The C−O* bond length using the pseudoatom compares well with the corresponding bond length in the full molecule for the *o*-methyl and *o*-ethyl pseudoatoms. One difficulty that arises in the parametrization of our ECP, as compared to work done by other authors, is generating an ECP that is capable of distinguishing between the two types of hydrogen in the reference cluster. Zhang et al.[16] and DiLabio et al.[17] used the ethane molecule where all six hydrogens are chemically equivalent; however, in DME the in-plane hydrogen (Figure 1) is distinct from the out-of-plane

TABLE 3: Comparison of Computed Bond Lengths (Å) and Angles (degrees) for Reference Molecules and Fragments with Pseudoatoms[a]

coordinate	*o*-methyl pseudoatom (dimethyl ether)	*o*-ethyl pseudoatom (methyl ethyl ether)
C−O*	1.414 (1.410)	1.410(1.411)
C−H(1)	1.089 (1.090)	1.089(1.090)
C−H(2)	1.096 (1.099)	1.091(1.098)
O−C−H(1)	110.1 (107.3)	105.7(107.3)
O*−C−H(1)−H(2)	120.3(119.4)	119.9(119.3)

[a] Values for the full molecules are in parentheses, and atom labels correspond to those shown in Figure 1.

TABLE 4: Computed Density Difference, as Defined by Equation 4, and Natural Charges for Fragments with Pseudoatoms and Full Molecules[a]

molecule	density difference	q(C)	q(H_1)	q(H_2)
dimethyl ether	.004	6.1 (6.2)	.86 (0.82)	.88 (0.85)
methyl ethyl ether	.003	6.1 (6.1)	.83 (0.79)	.83 (0.82)

[a] Values from full molecules are in parentheses.

hydrogens. The bond lengths between the two groups of hydrogen differ by 0.009 Å. This small difference is crucial and determines the preferential site for hydrogen atom extraction in our rate constant work. In the truncated cluster, all three hydrogen atoms are in essentially equivalent chemical environments as the only entity present to break the symmetry is the external charge field because the ECP is a spherically symmetric potential. As a result, the hydrogen bond lengths were heavily weighted during the optimization ($\omega = 10$ in eq 3 for the data points corresponding to the hydrogen bond lengths) of the ECP parameters to force convergence to a parameter set that gave distinct hydrogen bond lengths. Because of the heavy weighting of the hydrogen bond lengths, the O−C−H(1) angle, as shown in Table 3, of the in-plane hydrogen in the fragment is in error by ∼3° though the remaining internals show good agreement.

Table 4 shows two measures of the density of the fragments as compared to the full molecules. First, we report the normalized difference of the density with respect to the reference molecules, computed as

$$\frac{\sum_i [\rho^{\mathrm{ref}}(i) - \rho^{\mathrm{fragment}}(i)]^2}{\sum_i \rho^{\mathrm{ref}}(i)} \qquad (4)$$

where ρ^{ref} and ρ^{fragment} correspond to the full reference molecule and fragment plus pseudoatom densities at the ith point, respectively. The full density in the region of the methyl group is reproduced to less than one-half percent using the pseudoatom. In addition to the spatial analysis, we also report natural atomic charges for the carbon and hydrogen atoms contained in the fragment. The natural charge analysis,[27] which computes eigenvectors of atomic sub-blocks of the density matrix, is a more stringent test on the density than the Mulliken population analyses used previously.[16,17] The natural charges of the fragment compare well with the full molecule values.

Results

A. Structure and Transferability. Zhang et al.[16] found that their pseudoatom developed at the B3LYP level of theory transferred well to other methods including Hartree−Fock and BLYP. As a test of the transferability of the current method, we replaced an $O-CH_3$ unit in methyl ethyl ether and dimethoxymethane (Figure 2) with the *o*-methyl pseudoatom developed at the MP2 level and performed CCSD geometry optimizations of the fragments. It must be mentioned that in our scheme, the location of the charges in the external field is contingent upon analysis of the density resulting from the applied level of theory. We found, however, that the difference in location of the charges in the reference DME cluster for the MP2 and CCSD densities was negligible, as expected. Therefore, we used the MP2 orientation for all higher levels of correlation. A comparison of the CCSD geometries and CPU time required for the optimization of the fragments versus the full molecules is shown in Table 5. The MP2 pseudoatom performs well at the CCSD level of theory, and despite the significant reduction in size of the correlation space the error in geometry of the CCSD fragments is small. Also, as shown in Table 5, the slight geometric differences between hydrogens in different chemical environments (e.g., primary vs secondary hydrogens) are reproduced properly using the pseudoatom, the largest error being 0.2 picometers corresponding to the C(1)−H(1) bond in the dimethoxymethane system. It is important that this distinction be maintained by our truncation method because these small differences can have an impact on the kinetics of hydrogen atom abstraction. The computational speedups for the methyl ethyl ether and dimethoxymethane molecules using the pseudoatom are 7.9- and 9.1-fold, respectively.

In addition to transferability among levels of correlation, the transferability of the pseudoatoms to varying bond types was

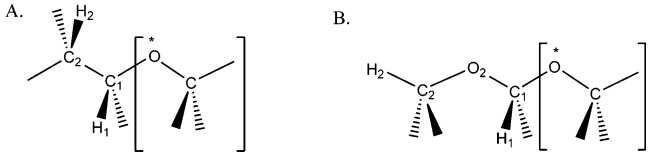

Figure 2. Methyl ethyl ether (A) and dimethoxymethane (B). Atoms in brackets are replaced by *o*-methyl pseudoatom.

TABLE 5: Comparison of Internal Coordinates/CPU Time for CCSD Level of Theory for Molecules Shown in Figure 2[a]

molecule	coordinate	value
A	O*−C(1)	1.434 (1.420)
A	C(1)−C(2)	1.505 (1.514)
A	C(1)−H(1)	1.096 (1.097)
A	C(2)−H(2)	1.090 (1.090)
A	C(1)−C(2)−H(2)	110.5 (110.2)
A	O*−C(1)−H(1)	108.4 (109.6)
A	O*−C(1)−C(2)	109.5 (108.2)
A	O*−C(1)−C(2)−H(2)	60.1(59.9)
A	H(1)−C(1)−C(2)−H(2)	59.5(60.3)
B	O*−C(1)	1.401(1.399)
B	C(1)−O(2)	1.382(1.398)
B	O(2)−C(2)	1.423(1.418)
B	C(1)−H(1)	1.101(1.103)
B	C(2)−H(2)	1.084(1.084)
B	O*−C(1)−O(2)	106.6(105.9)
B	C(1)−O(2)−C(2)	113.2(111.0)
B	O*−C(1)−H(1)	109.3(110.4)
B	H(1)−C(1)−O(2)−C(2)	60.4(60.3)
B	O*−C(1)−O(2)−C(2)	180.0(180.0)
	molecule	
	CPU time (s)	speedup
A	14344 (113542)	7.9 X
B	35466 (323209)	9.1 X

[a] Pseudoatom, denoted by O* in the table, uses the potential and charge field developed at the MP2 level. Values from full molecules are in parentheses. All computations run on IBM/SP3. Molecule A = methyl ethyl ether; B = dimethoxymethane. Bonds lengths in Angstroms, angles in degrees.

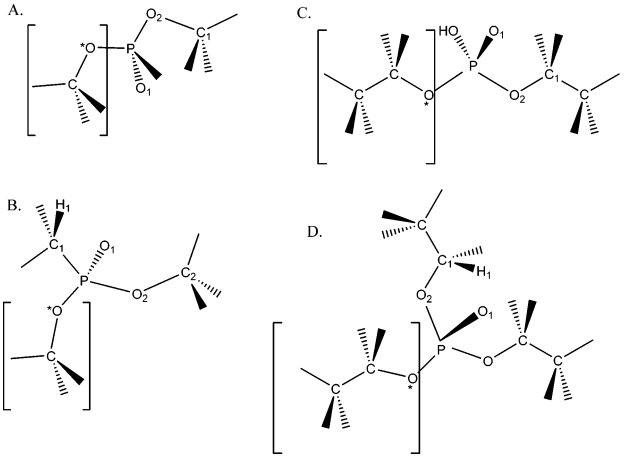

Figure 3. Geometries of (A) DMHP, (B) DMMP, (C) DEP, and (D) TEP. Atoms in brackets are replaced by pseudoatom.

also tested. Specifically, the ECP of the *o*-methyl/*o*-ethyl pseudoatoms were parametrized to yield the correct bond length with oxygen to which they were directly bonded in the reference clusters. As a test, we optimized the geometry of methoxy silane, H_3COSiH_3, where the methoxy unit was replaced with the *o*-methyl pseudoatom. The silicon−pseudoatom bond length computed at the MP2 level was found to be 1.662 Å, which compares well with the reference value of 1.673 Å found in the full molecule. This agreement is quite encouraging considering that this is an entirely different interaction for the pseudoatom.

In addition to reproducing the interaction with silicon properly, the pseudoatom also performs well for interactions with phosphorus. The *o*-methyl/*o*-ethyl pseudoatoms were used, where applicable, in optimizations of the set of phosphoethers shown in Figure 3, which include dimethyl phosphonate (DMHP), dimethyl methyl phosphonate (DMMP), diethyl phosphate (DEP), and triethyl phosphate (TEP). Values of the optimized internal coordinates are shown in Table 6 and show good agreement with the reference values from the full molecules. It should also be noted that the DMHP optimization was conducted at the MP4 level of theory using the pseudoatom parametrized at the MP2 level, yet the phosphorus-pseudoatom bond length is still in good agreement with the reference value. This serves as an additional example of transferability between methodology as well as bond type.

B. Energetics. As an assessment of the ability of the present scheme to reproduce energy differences properly, we report in Table 7 the deprotonation energies (MP2 and CCSD levels of theory) of each molecule contained in Figures 2 and 3. In all cases, one hydrogen atom attached to the C1 carbon was removed and the deprotonation energy using the psuedoatom-terminated cluster compared to that obtained using the full molecule. For methyl ethyl ether this is a particularly stringent test because the reactive site is only one bond removed from the pseudoatom. However, the errors for the MP2 and CCSD energies using the pseudoatom are only 0.6 and 1.3 kcal/mol, respectively, as compared to the values from the full methyl ethyl ether molecule. The pseudoatom performs well in all cases tested here, and the largest error corresponds to the CCSD deprotonation energy of the DEP molecule, which is still within 3.3 kcal/mol of the value obtained with the full molecule.

Conclusions

In this paper, an extension of the parametrized pseudoatom scheme was presented where the long-range Coulomb interaction of the truncated functional groups was modeled through an external charge field constructed via analysis of the electron density. The combination of parametrized ECP along with the external field provides results for minimum energy conformations, which show good agreement with values that result from treatment of the molecule in its entirety. The computational scaling, as shown for methyl ethyl ether, is reduced significantly because of the truncation of the molecule, and the pseudoatom shows good transferability between varying levels of electron correlation.

It should be mentioned that in addition to the minimum energy optimizations presented here, we have also done some preliminary work concerning the determination of transition-state

TABLE 6: Comparison of Internal Coordinates for Phoshphoethers Shown in Figure 3[a]

molecule	coordinate	value
A	O*−P	1.628(1.627)
A	P−O(1)	1.485(1.490)
A	P−O(2)	1.617(1.626)
A	O(2)−C(1)	1.463(1.453)
A	O*−P−O(1)	112.8(112.6)
A	O*−P−O(2)	101.9(105.2)
A	P−O(2)−C(1)	119.3(117.7)
A	O(1)−P−O*−O(2)	130.0(128.1)
A	O(1)−P−O(2)−C(1)	36.2(40.7)
B	O*−P	1.627(1.625)
B	P−O(1)	1.491(1.496)
B	P−O(2)	1.618(1.633)
B	P−C(1)	1.789(1.792)
B	O*−P−O(1)	115.7(115.8)
B	O*−P−O(2)	102.1(104.2)
B	P−O(2)−C(2)	119.3(119.1)
B	O(1)−P−O*−O(2)	124.0(125.1)
B	O(1)−P−C(1)−H(1)	176.1(177.0)
B	O*−P−C(1)−H(1)	56.1(56.2)
C	O*−P	1.599(1.601)
C	P−O(1)	1.483(1.492)
C	P−O(2)	1.583(1.601)
C	O(2)−C(1)	1.471(1.456)
C	O*−P−O(1)	118.8(118.3)
C	O*−P−O(2)	98.1(97.5)
C	P−O(2)−C(1)	118.2(117.7)
C	O(1)−P−O*−O(2)	130.7(127.9)
C	P−O(2)−C(1)−C	174.9(175.0)
C	O(1)−P−O(2)−C(1)	49.7(49.9)
D	O*−P	1.591(1.610)
D	P−O(1)	1.486(1.492)
D	P−O(2)	1.595(1.610)
D	O(2)−C(1)	1.471(1.456)
D	O*−P−O(1)	113.6(116.1)
D	O*−P−O(2)	105.1(102.1)
D	P−O(2)−C(1)	120.6(117.8)
D	O(1)−P−O*−O(2)	129.5(127.3)
D	O*−P−O(2)−C(1)	170.8(173.7)
D	O(1)−P−O(2)−C(1)	47.4(46.3)

[a] Values from full molecules are in parentheses. Molecule A = DMHP, B = DMMP, C = DEP, and D = TEP. Bond lengths in Angstroms, angles in degrees.

TABLE 7: Absolute Error (kcal/mol) for Deprotonation Energies of Molecules in Figures 2 and 3[a]

molecule	MP2	CCSD
methyl ethyl ether	.6	1.3
dimethoxymethane	.7	.8
DMHP	1.3	2.4
DMMP	1.7	1.8
DEP	2.0	3.3
TEP	.3	1.0

[a] The 6-31++G** basis was used in all cases except for the phosphoether CCSD calculations, which used the 6-31G basis.

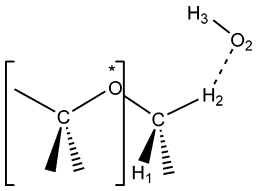

Figure 4. Transition state for hydrogen abstraction from DME. Atoms in brackets are replaced by pseudoatom.

TABLE 8: Comparison of Internal Coordinates for DME Transition State Shown in Figure 4[a]

coordinate	value
O*−C	1.404(1.397)
C−H(1)	1.094(1.096)
C−H(2)	1.189(1.191)
H(2)−O(2)	1.309(1.315)
O(2)−H(3)	0.968(0.969)
O*−C−H(1)	111.6(113.1)
O*−C−H(2)	110.2(105.6)
H(2)−O(2)−H(3)	97.6(95.1)
O*−C−H(1)−H(2)	116.0(115.5)

[a] Values for full molecule are in parentheses. Bond lengths in Angstroms, angles in degrees.

structures using the truncation method presented in this paper. As an example, Figure 4 shows one of the transition states for abstraction of a hydrogen from DME by the hydroxy radical. Replacing the methoxy unit not involved in the abstraction by the pseudoatom yields a transition-state structure that compares well with the configuration found in the full molecule (see Table 8). This transition state also lends further evidence in support of the importance of the point-charge field in the scheme presented here. It was found that if the parametrized ECP fluorine was used without inclusion of the long-range Coulomb interaction, then the hydroxy radical, in the truncated transition-state cluster, had the wrong orientation. As stated previously, the work on the transition state is preliminary and we have had some difficulty in applying the truncation methods to other transition-state structures successfully, although the results presented in Table 8 show promise. With further development, this technique appears to be a viable tool for reducing the computational cost for both equilibrium as well as transition-state structures.

Acknowledgment. D.E.T thanks the Research Associates Program sponsored by the National Academies for financial support and the Army Research Laboratory Major Shared Resource Center for computer access.

References and Notes

(1) Mallik, A.; Taylor, D. E.; Runge, K.; Dufty, J. W. *Int. J. Quantum Chem.* **2004**, *100*, 1019.
(2) Dixon, S. L.; Merz, K. M. *J. Chem. Phys.* **1996**, *104*, 6643.
(3) Millam, J. M.; Scuseria, G. E. *J. Chem. Phys.* **1997**, *106*, 5569.
(4) Bartlett, R. J.; Silver, D. M. *Chem. Phys. Lett.* **1974**, *29*, 199.
(5) Bartlett, R. J. In *Modern Electronic Structure Theory − Part II*; Yarkony, D. R., Ed.; World Scientific: Singapore, 1995.
(6) Flocke, N.; Bartlett, R. J. *J. Chem. Phys.* **2004**, *121*, 10935.
(7) Schutz, M.; Hetzer, G.; Werner, H. J. *J. Chem. Phys.* **1999**, *111*, 5691.
(8) Fedorov, D. G.; Kitaura, K. *J. Chem. Phys.* **2005**, *123*, 134103.
(9) Warshel, A.; Levitt, M. *J. Mol. Biol.* **1976**, *103*, 227.
(10) Vreven, T.; Morokuma, K.; Farkas, O.; Schlegel, H. B.; Frisch, M. J. *J. Comput. Chem.* **2003**, *24*, 760.
(11) Singh, U. C.; Kollman, P. A. *J. Comput. Chem.* **1986**, *7*, 718.
(12) Thery, V.; Rinaldi, D.; Rivail, J. L. *J. Comput. Chem.* **1994**, *15*, 269.
(13) Bessac, F.; Alary, F.; Carissan, Y.; Heully, J.; Daudey, J.; Poteau, R. *J. Mol. Struct.: THEOCHEM* **2003**, *632*, 43.
(14) Ferre, N.; Olivucci, M. *J. Mol. Struct.: THEOCHEM* **2003**, *632*, 71.
(15) Bakowies, D.; Thiel, W. *J. Phys. Chem.* **1996**, *100*, 10580.
(16) Zhang, Y.; Lee, T.; Yang, W. *J. Chem. Phys.* **1999**, *110*, 46.
(17) DiLabio, G.; Hurley, M. M.; Christiansen, P. *J. Chem. Phys.* **2002**, *116*, 9578.
(18) Vashishta, P.; Kalia, R. K.; Nakano, A. *J. Nanopart. Res.* **2003**, *5*, 119.
(19) Walsh, T. R.; Wilson, M.; Sutton, A. P. *J. Chem. Phys.* **2000**, *113*, 9191.
(20) DiLabio, G.; Wolkow, R. A.; Johnson, E. R. *J. Chem. Phys.* **2005**, *122*, 044708.
(21) de Leeuw, N. H.; Du, Z.; Li, J.; Yip, S.; Zhu, T. *Nano Lett.* **2003**, *3*, 1347.
(22) Bartlett, R. J.; Stanton, J. F. In *Reviews of Computational Chemistry*; Boyd, D., Lipkowitz, K., Eds.; VCH: New York, 1994.
(23) Stanton, J. F.; Gauss, J.; Watts, J. D.; Nooijen, M.; Oliphant, N.; Perera, S. A.; Szalay, P. G.; Lauderdale, W. J.; Kucharski, S. A.; Gwaltney, S. R.; Beck, S.; Balková, A.; Bernholdt, D. E.; Baeck, K. K.; Rozyczko, P.; Sekino, H.; Hober, C.; Bartlett, R. J. *ACES II*, a program product of the Quantum Theory Project, University of Florida. Integral packages included are VMOL (Almlöf, J.; Taylor, P. R.); VPROPS (Taylor, P.); ABACUS (Helgaker, T.; Jensen, H. J. Aa.; Jørgensen, P.; Olsen, J.; Taylor, P. R.).
(24) Zhang, Y. *J. Chem. Phys.* **2005**, *122*, 024114.
(25) Nocedal, J. *Math. Comput.* **1980**, *35*, 773.
(26) Charbonneau, P. *Astrophys. J. (Suppl.)* **1995**, *101*, 309.
(27) Reed, A. E.; Weinhold, F. *J. Chem. Phys.* **1985**, *83*, 735.